J. Biochem. 131, 97–105 (2002)

Development of a Synchronous Enzyme-Reaction System for a Highly Sensitive Enzyme Immunoassay[1]

Kuniyo Inouye,[2] Iori Ueno, Shin-ichi Yokoyama, and Toshiyuki Sakaki

Division of Food Science and Biotechnology, Graduate School of Agriculture, Kyoto University, Sakyo-ku, Kyoto 606-8502

Received August 16, 2001; accepted November 6, 2001

A synchronous enzyme-reaction system using water-soluble formazan and a non-enzymatic electron mediator was developed and applied to an enzyme immunoassay (EIA). The reaction system consists of four steps: (I) dephosphorylation of $NADP^+$ to produce NAD^+ by alkaline phosphatase (ALP), (II) reduction of NAD^+ to produce NADH with oxidation of ethanol to yield acetaldehyde by alcohol dehydrogenase (ADH), (III) reduction of water-soluble tetrazolium salt (WST-1) to produce formazan by NADH *via* 1-methoxy-5-methyl-phenazinium methyl sulfate (PMS), and (IV) re-reduction of NAD^+ to produce NADH by ADH. During each cycle, one molecule of tetrazolium is converted to one molecule of formazan. The concentration of formazan during the reaction was given by second-order polynomials of the reaction time. Kinetic studies strongly suggested that the synchronous enzyme-reaction system had the potential to detect an analyte at the attomole level in EIA. On the basis of the kinetic studies, optimal conditions for EIA incorporating the synchronous system were examined. $NADP^+$ was purified thoroughly to remove minor traces of NAD^+ in the preparation, and an ADH preparation contaminated with the lowest level of ALP activity was used. When the synchronous system was applied to a sandwich-type EIA for human C-reactive protein, the protein was detected with a sensitivity of 50 attomole per well of a micro-titer plate (0.1 ml) in a 1-h reaction. In addition, EIA with water-soluble formazan showed a more quantitative and sensitive result than that with insoluble formazan. These findings indicated that the (WST-1)-PMS system introduced in this study has a great potential for highly sensitive enzyme immunoassay.

Key words: clinical diagnosis, enzymatic cycling reaction, enzymatic sequential reaction, enzyme immunoassay, molecular synchronization, monoclonal antibody, synchronous enzyme-reaction system.

Enzyme immunoassay (EIA) is widely used for the measurement of a great variety of analytes such as drugs, hormones, tumour markers and environmental pollutants (*1, 2*). Although EIA has practical advantages, the sensitivity of EIA using colorimeters is often poor compared with that of radio-immunoassay and non-isotopic techniques employing fluorescence and luminescence. To enhance the sensitivity of EIA, we have applied modified or engineered antibodies such as active fragments of IgG and IgM monoclonal antibodies (mAbs) (*3–6*), bispecific antibodies (*7–9*), and (polymerized marker enzyme)-antibody conjugates (*7*). On the other hand, an enzyme-amplification system has been reported to overcome this limit to sensitivity of EIA (*10, 11*). The enzyme-amplification system involves the dephosphorylation of $NADP^+$ by alkaline phosphatase (ALP) to produce NAD^+, which catalytically activates a specific redox-cycle involving alcohol dehydrogenase (ADH) and diaphorase. During each cycle, one molecule of tetrazolium is reduced to one molecule of intensely colored formazan; and one molecule of NAD^+ generated by ALP can catalyze the production of a number of molecules of formazan dye (*12–16*). Thus, the enzyme amplification can increase the sensitivity by 100–1,000-fold as compared with non-amplified methods (*10, 12*). Although an amplification system using a water-insoluble tetrazolium (INT) and diaphorase is now commercially available, the quantitative determination of analytes has been often disturbed by production of insoluble formazan. In this paper, the use of a water-soluble tetrazolium salt (WST-1) (*17, 18*) instead of INT was examined. In addition, PMS, which is a versatile non-enzymatic electron mediator between NAD(P)H and tetrazolium (*19–21*), was used instead of diaphorase, since the greater stability of PMS was expected to allow a longer-term reaction resulting in higher sensitivity. The EIA system proposed in this study is composed of the conventional sandwich-type

[1] This work was supported in part (K.I.) by Grants-in-Aid for Scientific Research on Priority Areas (A) (Nos. 11167248 and 13022236) from the Ministry of Education, Culture, Sports, Science and Technology of Japan.

[2] To whom correspondence should be addressed. Phone: +81-75-753-6266, Fax: +81-75-753-6265; E-mail: inouye@kais.kyoto-u.ac.jp

Abbreviations: ADH, alcohol dehydrogenase; ALP, alkaline phosphatase; CRP, C-reactive protein; EIA, enzyme immunoassay; HEPES, 2-[4-(2-hydroxyethyl)-1-piperazinyl]ethanesulfonic acid; INT, 2-(4-iodophenyl)-3-(4-nitrophenyl)-5-phenyl-2*H* tetrazolium chloride; mAb, monoclonal antibody; PMS, 1-methoxy-5-methylphenazinium methyl sulfate; Tween 20, polyoxyethylene (20) sorbitan monolaurate; WST-1, 2-(4-iodophenyl)-3-(4-nitrophenyl)-5-(2,4-disulfophenyl)-2*H*-tetrazolium, monosodium salt.

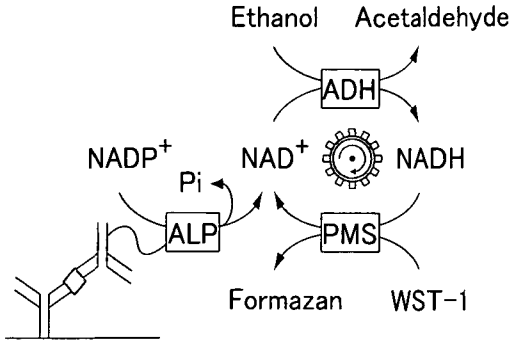

Fig. 1. **Scheme for a sandwich-type EIA system incorporating the (WST-1)-PMS synchronous enzyme reactions.** ALP, alkaline phosphatase; ADH, alcohol dehydrogenase; PMS, 1-methoxy-5-methylphenazinium methyl sulfate; and WST-1, a water-soluble tetrazolium salt.

EIA and the synchronous enzyme-reactions using WST-1 and PMS as shown in Fig. 1. The (WST-1)-PMS synchronous enzyme-reaction system is kinetically analyzed, and its practical application to a highly sensitive EIA of human C-reactive protein (CRP) is demonstrated.

MATERIALS AND METHODS

Kinetic Theory—Kinetic analysis of the enzymic cycling system using INT and diaphorase was reported by Valero *et al.* (*13*). In this study, their kinetic theory was applied to the (WST-1)-PMS synchronous enzyme-reaction system. The synchronous system is described as follows:

$$S_1 \xrightarrow{E_1} X \quad (1)$$

$$S_2 + X \xrightarrow{E_2} Y + P_1 \quad (2)$$

$$S_3 + Y \xrightarrow{E_3} Z + X \quad (3)$$

where S_1, S_2, S_3, and P_1 represent NADP$^+$, ethanol, WST-1, and acetaldehyde, respectively; X, Y, and Z are NAD$^+$, NADH and formazan respectively; and E_1, E_2, and E_3 are alkaline phosphatase (ALP), alcohol dehydrogenase (ADH) and PMS, respectively. Reaction 3 consists of two oxido-reduction reactions described below.

$$PMSox + Y \xrightarrow{k_X} X + PMSred \quad (4)$$

$$PMSred + S_3 \xrightarrow{k_Z} Z + PMSox \quad (5)$$

where PMSox and PMSred represent the oxidized PMS and the reduced PMS, respectively, and k_X and k_Z are the rate constants of reactions 4 and 5, respectively. In reaction 3, the conversion rate of the reduced PMS to oxidized PMS can be approximated to zero if the WST-1 and PMS concentrations are in large excess of NADH concentration (steady-state approximation):

$$\frac{d[PMSred]}{dt} = k_X[PMSox]Y - k_Z[PMSred][S_3] \approx 0 \quad (6)$$

Thus, the rate of the formazan (Z) formation is given by:

$$\frac{dZ}{dt} = k_Z[PMSred][S_3] \approx k_X[PMSox]Y \approx k_X[PMS]_0Y \quad (7)$$

The following kinetic equations are deduced from reactions formulas 1–3.

$$\frac{dX}{dt} = \frac{k_1[E_1]_0S_1}{K_{m1} + S_1} - \frac{k_2'[E_2]_0X}{K_{m2} + X} + k_3'[E_3]_0Y \quad (8)$$

$$\frac{dY}{dt} = \frac{k_2'[E_2]_0X}{K_{m2} + X} - k_2'[E_2]_0Y \quad (9)$$

$$\frac{dZ}{dt} = k_3'[E_3]_0Y \quad (10)$$

where k_1, k_2' and k_3' are the rate constants of Eqs. 1–3, respectively. K_{m1} is the Michaelis constant of NADP$^+$ (S_1) towards ALP (E_1). K_{m2} is the Michaelis constant of NAD$^+$ (X) towards ADH (E_2) as a function of the ethanol (S_2) concentration. As S_2 is in the saturating level, K_{m2} is nearly equal to K_{mx}, which is the Michaelis constant of X towards E_2. The concentration of S_1 can be set higher than the Michaelis constant K_{m1}, and the concentration of S_2 is high enough to be saturating. Accordingly, the concentration of X is considered to be lower than K_{m2} during the reaction. Under these conditions, Eqs. 8–10 can be simplified as:

$$\frac{dX}{dt} = V_1 - k_2X + k_3Y \quad (11)$$

$$\frac{dY}{dt} = k_2X - k_3Y \quad (12)$$

$$\frac{dZ}{dt} = k_3Y \quad (13)$$

where $V_1 = k_1[ALP]_0$, $k_2 = \frac{k_2'C}{K_{m2}}[ADH]_0$, and $k_3 = k_3'[PMS]_0$, respectively. Solving Eqs. 11–13, the formazan concentration (Z) is represented by:

$$Z = k_3\left\{\frac{k_2\left(V_1 - \lambda X_0\right)}{\lambda^3}\left(1 - e^{-\lambda t}\right) + \frac{k_2V_1}{2\lambda}t^2 - \frac{k_2\left(V_1 - \lambda X_0\right)}{\lambda^2}t\right\} \quad (14)$$

where $\lambda = k_2 + k_3$.

In the steady-state conditions ($t \to \infty$), the exponential term ($e^{-\lambda t}$) in Eq. 14 is negligible, and the equation can be simplified as:

$$Z = k_3\left\{\frac{k_2V_1}{2\lambda}t^2 - \frac{k_2\left(V_1 - \lambda X_0\right)}{\lambda^2}t + \frac{k_2\left(V_1 - \lambda X_0\right)}{\lambda^3}\right\} \quad (15)$$

Evaluation of k_2 and k_3—In the NAD$^+$ cycling reaction system not containing ALP, V_1 is zero in Eq. 15. Thus, the concentration of formazan at time t is represented by:

$$Z = k_3\left(\frac{k_2X_0}{\lambda}t - \frac{k_2X_0}{\lambda^2}\right) \quad (16)$$

Thus, the rate of formazan formation is given by:

$$\frac{dZ}{dt} = \frac{k_2k_3}{k_2 + k_3}X_0 = kX_0 \quad (17)$$

where $k = \frac{k_2k_3}{k_2 + k_3}$ (18)

Equation 18 can be transformed to:

$$\frac{1}{k} = \frac{1}{k_2} + \frac{1}{k_3} \quad (19)$$

Inserting $k_2 = \frac{k_2'}{K_{m2}}[ADH]_0$ and $k_3 = k_3'[PMS]_0$ into Eq. 19, we obtain:

$$\frac{1}{k} = \frac{1}{k_2} + \frac{1}{k_3'}\frac{1}{[PMS]_0} \quad (20)$$

$$\frac{1}{k} = \frac{K_{m2}}{k_2'}\frac{1}{[ADH]_0} + \frac{1}{k_3} \quad (21)$$

Thus, k_2 and k_3 will be obtained by plotting $1/k$ *versus* $1/[PMS]_0$ and $1/k$ *versus* $1/[ADH]_0$, respectively.

Evaluation of k_1—Equation 15 is transformed to:

$$dZ/dt = k_2k_3(V_1 t - V_1/\lambda - X_0)/\lambda = k_1k_2k_3[ALP]/(k_2 + k_3) \quad (22)$$

Here, we define the acceleration factor (A) as the slope of the plot of dZ/dt against the ALP concentration:

$$A = \frac{k_1k_2k_3}{k_2 + k_3}[ALP]_0 \quad (23)$$

Thus, k_1 will be obtained by plotting A against [ALP] and inserting the k_2 and k_3 values described in the last paragraph.

Materials—ALP [EC 3.1.3.1] (Lots 53204801 and 53205901) from calf intestine, ADH [EC 1.1.1.1] (Lots 20001004, 20001903, and 20005904) from yeast, diaphorase [EC 1.6.99.1] (Lots 50403803 and 50403003) from *Clostridium kluyveri*, β-$NADP^+$ (Lot 040912), β-NAD^+ (Lot 7901), and NADH (Lot 10340) were obtained from Oriental Yeast (Tokyo). PMS (Lot FA036), INT (Lot DX108), and WST-1 (Lot FC078) were obtained from Dojindo (Kumamoto). Human CRP (Lot B-7) was obtained from F. Hoffmann-La Roche (Basel, Switzerland). Bovine serum albumin (BSA), EIA/RIA grade, essentially globulin-free, was purchased from Nacalai Tesque (Kyoto). Disodium *p*-nitrophenyl-phosphate (PNPP) hexahydrate was from Wako Pure Chemicals (Osaka). All other chemicals were purchased from Nacalai Tesque (Kyoto).

Antibodies—A mouse hybridoma cell line producing monoclonal antibody (mAb) CR982 of IgG1 class was established in our laboratory by fusing spleen cells from an antigen (CRP)-immunized BALB/c mouse with NS-1 myeloma cells. The hybridoma cells were injected into pristane-primed BALB/c mice and grown in ascites. Ascitic fluids containing mAb CR982 were prepared, and the mAb was purified to homogeneity by SDS-PAGE (*3, 22, 23*). Anti–human CRP sheep polyclonal antibody conjugated with highly pure ALP was obtained from Biogenesis (London, UK). Concentrations of proteins were determined by the method of Lowry *et al.* (*24*) using BSA as the standard, and that of the purified mAb was determined spectrophotometrically using an absorption coefficient at 280 nm of A_{280} (1 mg/ml) = 1.4 (*3*).

Cycling Assay with ALP and $NADP^+$—The reaction was carried out at 25°C in 100 mM Tris-HCl buffer, pH 8.5, containing 8 mM $MgCl_2$ (buffer A). WST-1, PMS, ethanol, ALP, and ADH were added to the buffer in a cuvette to give final concentrations of 100 μM, 5 μM, 260 mM, 0–8 ng/ml, and 0.54 μM, respectively. At 45 s after the addition of ADH, the reaction was started by addition of $NADP^+$ at the final concentration of 250 μM. From 15 s after the $NADP^+$ addition, the absorbance change at 438 nm was continuously monitored.

Cycling Assay with NAD^+—WST-1, PMS, ethanol, and ADH were added to buffer A at 25°C in a cuvette to give final concentrations of 100 μM, 5–100 μM, 260 mM, and 0.136–1.09 μM, respectively. At 45 s after the ADH addition, the reaction was started by addition of NAD^+ at the final concentration of 0.2 μM. From 15 s after the NAD^+ addition, the absorbance change at 438 nm was continuously monitored. For calculation of k_2, [ADH] was kept constant at 0.54 μM and [PMS] was varied from 5 to 100 μM. For calculation of k_3, [PMS] was kept constant at 5 μM and [ADH] was varied from 0.136 to 1.09 μM.

Purification of $NADP^+$ by High-Performance Liquid Chromatography (HPLC)—The $NADP^+$ solution was purified by HPLC on a LiChrosorb RP-8 column [4 mm (inner diameter) × 12.5 cm] (Cica-Merck, Tokyo). The sample was injected into the column equilibrated with the elution buffer [acetonitrile: 10 mM Bis-Tris buffer (pH 6.5) containing 1 mM tetra-*n*-butyl ammonium hydrogen sulfate (10:90 v/v)]. Elution was carried out with the elution buffer at a flow-rate of 1.0 ml/min. The column temperature was maintained at 25°C. The eluate was monitored by measuring absorbance at 254 nm. The purified $NADP^+$ fraction was dried up and stored at –20°C.

EIA—Anti-CRP monoclonal antibody (mAb CR982) was adsorbed onto a well of a micro-titer plate (Maxi Sorp, Nunc-Intermed, Roskilde, Denmark) by incubation at 37°C for 2 h at 100 μg/ml in 100 μl of 20 mM HEPES, pH 7.4, containing 150 mM NaCl (buffer B). The well was washed three times with 250 μl of buffer B containing 0.05% Tween 20 (washing buffer), then blocked with BSA by addition of 250 μl of 10 mg/ml BSA and incubation for 15 h at 4°C. After washing the well three times with the washing buffer, 100 μl of the CRP solution was added and incubated for 2 h at 37°C. The well was again washed three times with the washing buffer, then the anti-CRP antibody labeled with ALP at 100 ng/ml in 100 μl of buffer B containing 1 mg/ml BSA was added and incubated at 37°C for 2 h. Unbound antibody was removed by washing four times with 250 μl AmpliQ wash buffer (Dako A/S, Glostrup, Denmark). The ALP activity bound to the well was measured by the enzyme-amplifying procedure. After addition of the amplifier solution (100 μl), absorbance at 450 nm was measured against the reference absorbance at 600 nm by using a MPR-A4 titer plate reader (Tosoh, Tokyo). Amplifier solution (I) for the (WST-1)-PMS system contained 50 μM $NADP^+$, 1.6 μM ADH, 260 mM ethanol, 200 μM PMS, and 200 μM WST-1 in buffer A; and amplifier solution (II) for the INT-diaphorase system contained 50 μM $NADP^+$, 1.6 μM ADH, 260 mM ethanol, 65 μg/ml diaphorase, and 500 μM INT in buffer A.

Determination of the ALP Activity—The ALP activity was determined by measuring the production of *p*-nitrophenol by hydrolysis of 2.5 mM p-nitrophenylphosphate (PNPP) at 25°C in buffer A. *p*-Nitrophenol was determined by the change of absorbance at 405 nm by using the molar absorption coefficient of $\Delta\varepsilon_{405} = 1.84 \times 10^4\ M^{-1}\ cm^{-1}$ at pH 8.5.

Other Methods—Absorption spectrophotometric measurements were made with a Shimadzu UV-2200 recording spectrophotometer (Kyoto). The concentration of ALP was estimated from its molecular weight of 54,700 (*25*) assuming the 100% purity of the ALP preparation. The concentration of ADH was determined spectrophotometrically using the absorption coefficient of A_{280} (1 mg/ml) = 1.26 (*26*) on

the basis of the molecular weight of 36,800 (*27*). The concentration of diaphorase was determined with the following equation: dilution × (A_{280} × 1.45–A_{260} × 0.74) = mg/ml protein (*28*). The concentrations of PMS, WST-1 and formazan were determined spectrophotometrically using the molar absorptivities at pH 8.5 of ε_{505} = 2.84 × 10^3 M^{-1} cm^{-1}, ε_{244} = 2.30 × 10^4 $M^{-1}cm^{-1}$, and ε_{438} = 3.87 × 10^4 M^{-1} cm^{-1}, respectively (*17*). The concentrations of $NADP^+$, NAD^+, and NADH were determined using the molar absorptivities of ε_{259} = 1.80 × 10^4 M^{-1} cm^{-1} (pH 7.5), ε_{260} = 1.77 × 10^4 M^{-1} cm^{-1} (pH 7.5), and ε_{340} = 6.10 × 10^3 M^{-1} cm^{-1} (pH 8.5), respectively.

RESULTS

Cycling Assay with ALP and $NADP^+$—Figure 2 shows the time-courses of formazan formation at various ALP concentrations under the conditions described in "MATERIALS AND METHODS." Each curve was shown to be parabolic, as expected from Eq. 15. From Eq. 15, the formazan concentration should be zero when the initial concentrations of ALP and NAD^+ are zero. However, significant formation of formazan was observed in the absence of ALP. This suggests contamination by NAD^+ at a level of 0.1% in the commercially available $NADP^+$ preparation used (*13*).

Evaluation of k_2 and k_3—Formazan formation was measured at various concentrations of PMS and ADH in the presence of 0.2 μM NAD^+ as described in the paragraph of cycling assay with NAD^+ in "MATERIALS AND METHODS." The rate constant k was determined from the initial rate of the formazan production (Eq. 17). The rate constants k_2 and k_3 were determined from double-reciprocal plots of k *versus* [PMS] and k *versus* [ADH], respectively (Fig. 3). Values of k_2 = 48.1 min^{-1} at 0.54 μM ADH and k_3 = 2.14 min^{-1} at 5 μM PMS were obtained. The rate constant [$k = k_2k_3/(k_2 + k_3)$] of the NAD^+ cycling reaction, which was designated as the number of formazan molecules formed from one NAD^+ molecule in one min, was calculated to be 2.05 min^{-1}.

Evaluation of k_1—The first derivative (dZ/dt) for each curve at different ALP concentrations in Fig. 2 was plotted against the reaction time (t) (Fig. 4A). The acceleration A [= $k_1k_2k_3[ALP]_0/(k_2+k_3)$] calculated from the slope of the plot (dZ/dt) *versus* t was plotted against [ALP] (Fig. 4B). The rate constant k_1 was determined to be 7.17 × 10^3 min^{-1} from the slope of Fig. 4B and the k_2 and k_3 values obtained above.

Evaluation of the Michaelis Constant (K_{m1}) of $NADP^+$ towards ALP—The theoretical formulas cited in the Kinetic Theory section rest on the assumptions that: the concentration of S_1 is higher than the Michaelis constant K_{m1} of $NADP^+$ towards ALP; the concentration of S_2 is high enough to be saturating during the reaction; and the concentration of X is lower than the Michaelis constant K_{m2} and nearly equal to K_{mx}. The K_m values obtained proved that the concentrations used in the cycling assay fulfilled these conditions. Equation 23 is converted as follows at non-saturating concentration of $[NADP^+]_0$.

$$A = \frac{k_3k_3}{k_2 + k_3} \cdot k_1[\mathrm{ALP}]_0 = k \cdot \frac{k_1[\mathrm{ALP}]_0[\mathrm{NADP}^+]_0}{K_{m1} + [\mathrm{NADP}^+]_0} = k \cdot \frac{V_1[\mathrm{NADP}^+]_0}{K_{m1} + [\mathrm{NADP}^+]_0} \quad (24)$$

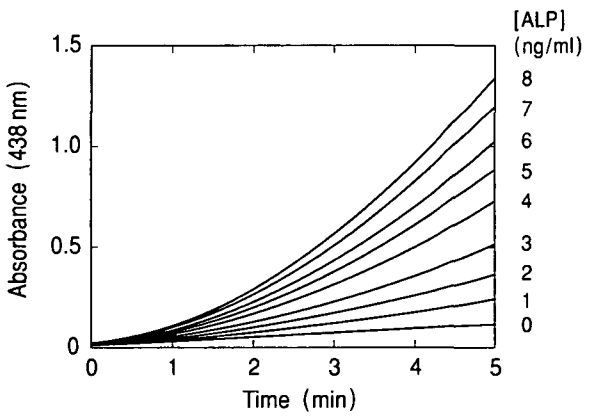

Fig. 2. **Time-courses of formazan formation catalyzed by various concentrations of ALP.** The absorbance change at 438 nm was continuously monitored in 100 mM Tris-HCl buffer (pH 8.5) containing 8 mM $MgCl_2$ (buffer A) at 25°C with 250 μM $NADP^+$, 0.54 μM ADH, 5 μM PMS, 100 μM WST-1, 260 mM ethanol, and 0–8 ng/ml ALP. If the ALP preparation is 100% pure, 1 ng/ml ALP corresponds to 18 pM ALP.

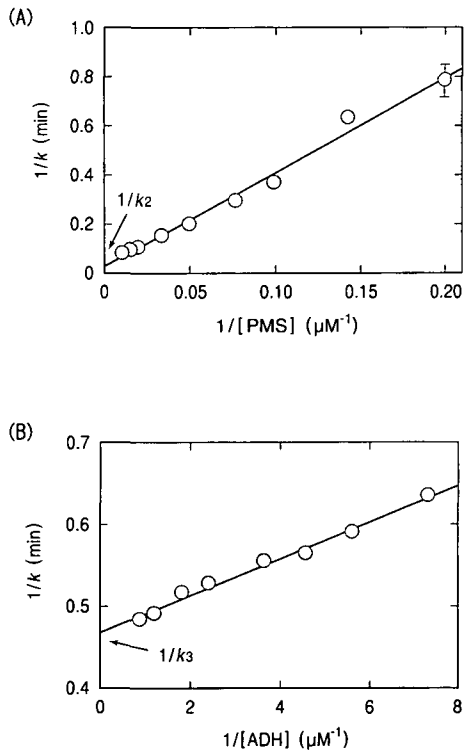

Fig. 3. **Evaluation of the rate constants (k_2 and k_3) for the ADH and PMS reactions, respectively.** Panel A: Evaluation of k_2. Formazan formation was measured in buffer A at 25°C with 0.2 μM NAD^+, 0.54 μM ADH, 5–100 μM PMS, 100 μM WST-1, and 260 mM ethanol. The k_2 value was calculated to be 48.1 min^{-1} according to Eq. 20. Panel B: Evaluation of k_3. Formazan formation was measured in buffer A at 25°C with 0.2 μM NAD^+, 0.136–1.09 μM ADH, 5 μM PMS, 100 μM WST-1, and 260 mM ethanol. The k_3 value was calculated to be 2.14 min^{-1} according to Eq. 21.

$$A/k = \frac{V_3[\mathrm{NADP^+}]_0}{K_{m1} + [\mathrm{NADP^+}]_0} \quad (25)$$

Formazan production was measured at different $NADP^+$ concentrations with 0 or 5 ng/ml ALP. As the reaction was also observed with 0 ng/ml ALP, the acceleration (A) was obtained by subtracting each curve at 0 ng/ml ALP from that at 5 ng/ml ALP. The K_{m1} value was estimated to be 39.2 μM from the plot of $[NADP^+]/(A/k)$ against $[NADP^+]$ (Hanes-Woolf plot) for the Michaelis-Menten type formula of Eq. 25, where the k value obtained above (2.05 min^{-1}) was used. Thus, it was confirmed that 250 μM $NADP^+$ used in the cycling assay is much higher than the K_{m1} value.

Evaluation of the Michaelis Constants of Ethanol (K_{ms2}) and NAD^+ (K_{mx}) towards ADH—The Michaelis constants K_{ms2} and K_{mx} were determined separately from Hanes-Woolf plots (data not shown) to be 7.78 mM and 82.8 μM, respectively. Thus, it was confirmed that 260 mM ethanol used in the cycling assay was much higher than the K_{ms2} value. On the other hand, the NAD^+ concentration in the cycling assay appeared much lower than the K_{mx} value.

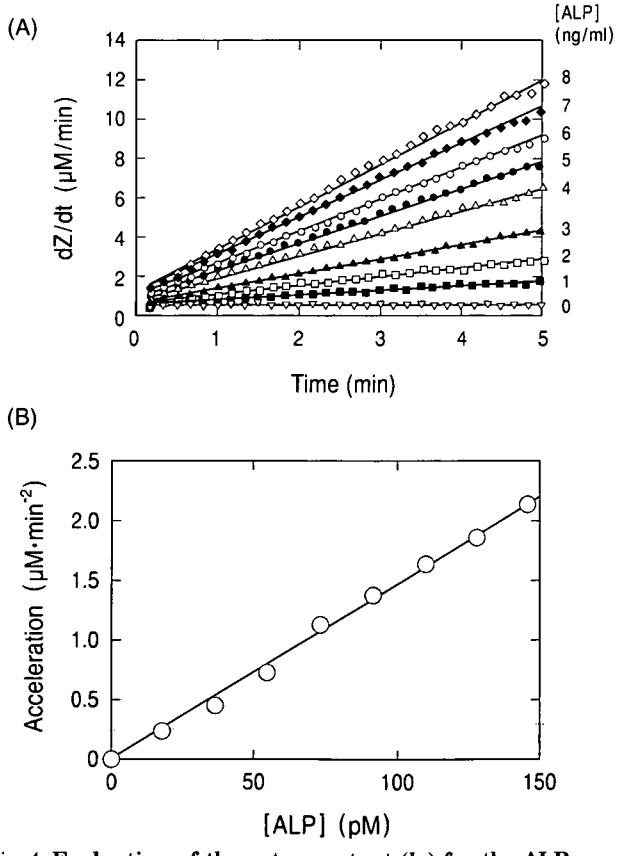

Fig. 4. **Evaluation of the rate constant (k_1) for the ALP reaction.** Panel A: Dependence of the first derivative (dZ/dt) of the formazan formation observed in Fig. 2 on the reaction time (t). Here, Z represents the amount of formazan formed at time t, thus dZ/dt represents the rate of formazan formation at time t. The acceleration (A) value at each ALP concentration was determined from the slope of the line. Panel B: Dependence of the acceleration A on the ALP concentration. The k_1 value was determined to be 7.17×10^3 min^{-1} from the slope $[= k_1k_2k_3/(k_2 + k_3)]$ of 1.47×10^4 min^{-2} according to Eq. 23.

Purification of $NADP^+$ with HPLC—The $NADP^+$ solution prepared from the commercially available $NADP^+$ preparation at the concentration of 10 mg/ml in 10 mM Bis-Tris buffer (pH 6.5) was analyzed by HPLC under the conditions described in "MATERIALS AND METHODS" (data not shown). A minor peak of NAD^+ in addition to a major peak of $NADP^+$ was observed. NAD^+ and $NADP^+$ eluted at 3.0 min and 5–10 min, respectively, and were clearly separated. The amount of NAD^+ contaminating in the $NADP^+$ preparation was estimated to be 0.01% or less by comparing their peak areas. The time-course of formazan formation by the cycling assay with the HPLC-purified $NADP^+$ preparation was compared with that of the commercially available $NADP^+$ preparation. The background due to the contaminating NAD^+ in the $NADP^+$ preparation used was reduced to less than 10%. The purified $NADP^+$ preparation was used in the following experiments.

Determination of the Optimum Conditions in the Cycling Reaction for EIA—(1) $NADP^+$ concentration: The residual background in the formazan formation observed with the HPLC-purified $NADP^+$ preparation was still high for highly sensitive EIA. The background observed with 50 μM $NADP^+$ decreased to 23% of that with 250 μM $NADP^+$, while the dephosphorylation activity of ALP decreased to only 61%. Thus, the optimal $NADP^+$ concentration for EIA was set at 50 μM. (2) PMS and ADH concentrations: The k_2 and k_3 values were expected to increase in proportion to [ADH] and [PMS] according to the equations $k_2 = \frac{k_2'}{K_{m2}}[\mathrm{ADH}]_0$ and $k_3 = k_3'[\mathrm{PMS}]_0$, respectively. However, the rate of formazan formation in the presence of NAD^+ was maximal at 200 μM PMS and decreased at higher concentrations (Fig. 5). This suggests an inhibitory effect of PMS on the ADH activity. The rate of formazan formation decreased with increasing [PMS] from 200 to 500 μM. The inhibition of ADH by PMS was examined at two different NAD^+ concentrations. The inhibition mode was shown to be competitive, and the inhibitor constant, K_i, was determined to be 145 μM by plotting ($1/v$) against [PMS] (Dixon plot for determining K_i) (*29*) (data not shown). Accordingly, the inhibitory effect of PMS on the ADH activity can be neglected when [PMS] is less than 50 μM, as shown in Fig. 3A. The possibility that PMS could be a substrate of ADH was also examined (*30, 31*). Formazan was formed even in

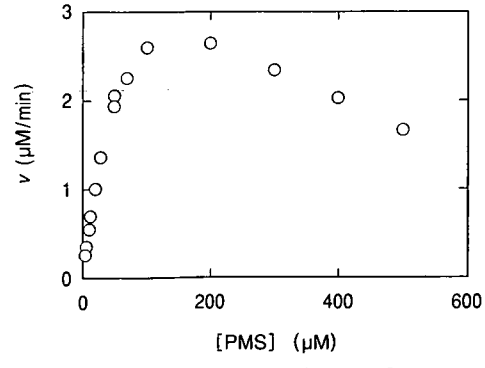

Fig. 5. **Effect of the PMS concentration on the rate of formazan formation.** Formazan formation was measured in buffer A at 25°C with 0.2 μM NAD^+, 0.54 μM ADH, 5–500 μM PMS, 100 μM WST-1, and 260 mM ethanol.

the absence of NAD^+, indicating that PMS is reduced by ADH, although the rate is extremely low (0.1% of the activity observed with NAD^+). Therefore, PMS is regarded as a competitive inhibitor of ADH, for which it competes with NAD^+. The Michaelis constant of PMS was estimated to be 82.9 μM by plotting [PMS]/v against [PMS] (Hanes-Woolf plot) (data not shown), suggesting that PMS had the same affinity as NAD^+ (K_m = 82.8 μM). From these lines of evidence, the optimum concentration of PMS for EIA was set at 200 μM. In order to find the optimum concentration of ADH, the effect of the ADH concentration on the reaction rate in the presence of 200 μM PMS was examined. The reaction rate reached the maximum at 1.6 μM ADH (Fig. 6).

Evaluation of k at 200 μM PMS and 1.6 μM ADH—It was found that the k_3 value was not proportional to [PMS] due to the inhibitory effect of PMS on the ADH activity. The rate constant k_3 at 200 μM PMS was estimated to be 26.3 min^{-1} from double-reciprocal plots, 1/k *vs.* 1/[ADH] (data not shown). In the presence of 200 μM PMS and 1.6 μM ADH, the k value was calculated to be 18.6 min^{-1}, which was about nine times larger than that obtained with 5 μM PMS and 0.54 μM ADH. On the basis of the k_3 and k values, the k_2 value was calculated to be 63.5 min^{-1}.

EIA Incorporating the Synchronous Enzyme-Reaction Systems—A sandwich EIA for CRP was performed using the (WST-1)-PMS system, and Fig. 7 shows the time-course of formazan formation in the EIA. The formazan formation showed a sigmoid curve consisting of a quadratic curve at the initial step of reaction according to Eq. 15, then a straight line after all $NADP^+$ had been transformed into NAD^+ (V_1 = 0, $dZ/dt = [NAD^+]_0/\lambda$), and finally an asymptote up to complete conversion of WST-1 into formazan (k_3 = 0, dZ/dt = 0). The sigmoid curve was observed even in the absence of CRP. Formazan formation was measured in the presence of the ALP-conjugated antibody and the amplifier solution on the plate blocked with BSA, and also in the presence of only the amplifier solution on the unblocked plate. In both cases, the time-courses of formazan formation appeared identical. This suggests that the non-specific binding of the ALP-conjugated antibody to the plate was prevented by the blocking with BSA, and that the amplifier solution might contain ALP activity. The ALP activity of the amplifier solution was therefore measured with PNPP as a substrate in the presence of PMS or ADH. The ADH solution (200 μg/ml) exhibited ALP activity equal to 1.75 ng/ml of ALP, while PMS showed no ALP activity, strongly suggesting that the commercially available ADH preparation included ALP as a contaminant at a level of 0.001%. When formazan formation was measured on a BSA-blocked plate with immobilized mAb CR982 in the presence of the ALP-conjugated antibody and the amplifier solution, the formation of formazan was enhanced in comparison with that on the plate without immobilized mAb CR982. This suggests direct binding of the ALP-conjugated antibody to the immobilized mAb CR982. Thus, it was found that the background observed at [CRP] of zero originated from the ALP activity present in the amplifier solution and the non-specific binding of the ALP-conjugated antibody to the immobilized antibody. Figure 8 shows standard curves for CRP at the reaction times of 31 and 61 min. In both cases, the for-

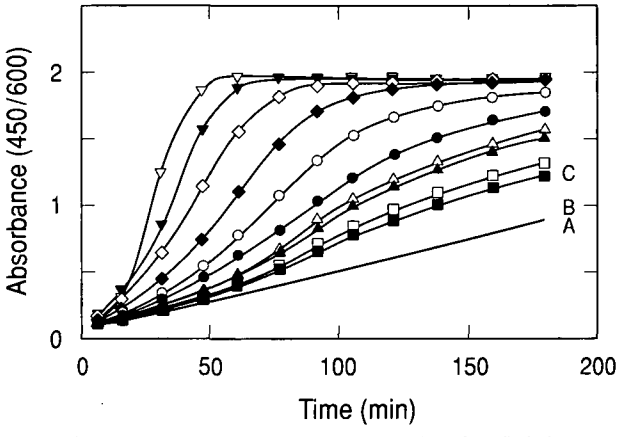

Fig. 7. **Time-courses of formazan formation by EIA incorporating the (WST-1)-PMS synchronous system for the detection of CRP.** The reaction was carried out in buffer A with 50 μM $NADP^+$, 1.6 μM ADH, 260 mM ethanol, 200 μM WST-1, and 200 μM PMS. The CRP concentrations are 48 (▽), 24 (▼), 12 (◇), 6 (◆), 3 (○), 1.5 (●), 0.74 (△), 0.37 (▲), 0.19 (□), and 0 (■) pM. The background formazan formation was measured under three different conditions without CRP. A: in the presence of the ALP-conjugated antibody and the amplifier solution on the plate blocked with BSA; B: in the presence of the amplifier solution on the plate not blocked; and C: in the presence of the ALP-conjugated antibody and the amplifier solution on the plate with immobilized mAb CR982 and blocked with BSA.

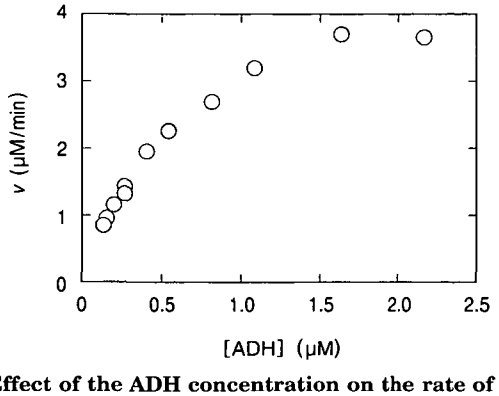

Fig. 6. **Effect of the ADH concentration on the rate of formazan formation.** Formazan formation was measured in buffer A at 25°C with 0.2 μM NAD^+, 0.136–2.17 μM ADH, 200 μM PMS, 100 μM WST-1, and 260 mM ethanol.

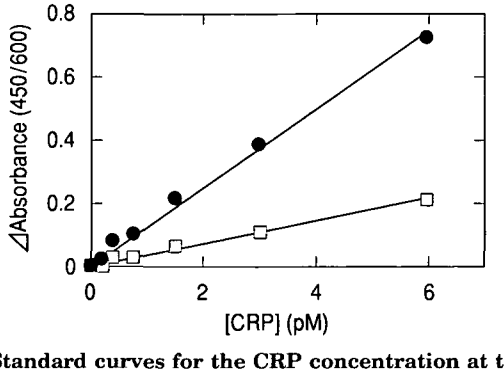

Fig. 8. **Standard curves for the CRP concentration at the reaction times of 31 (□) and 61 (■) min by EIA incorporating the (WST-1)-PMS system.** The CRP concentration was in the range of 0–8 pM, and the sample volume was 0.1 ml.

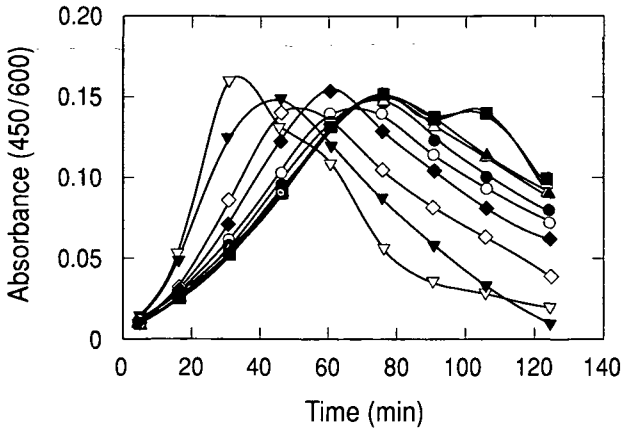

Fig. 9. **Time-courses of formazan formation by EIA incorporating the INT-diaphorase system for detection of CRP.** The reaction was carried out in buffer A with 50 μM $NADP^+$, 1.6 μM ADH, 260 mM ethanol, 500 μM INT, and 65 μg/ml diaphorase. The CRP concentrations are 48 (▽), 24 (▼), 12 (◇), 6 (◆), 3 (○), 1.5 (●), 0.74 (△), 0.37 (▲), 0.19 (□), and 0 (■) pM.

mazan concentration formed in the reaction mixture increased linearly with the increase in [CRP] from 0.1 to 6 pM, and the detection limit of CRP was safely evaluated to be 0.5 pM (50 attomole in 0.1 ml).

Comparative Analysis of the EIA Incorporating the INT-Diaphorase Synchronous System—To evaluate the EIA incorporating the cycling system using diaphorase and INT, we examined formazan formation at various CRP concentrations in EIA incorporating the INT-diaphorase synchronous system (Fig. 9). The absorbance change increased to the maximum level of 0.14–0.16 during the reaction, and then decreased. The time required to reach the maximum absorbance change decreased from 70 min to 30 min with the increase in the CRP concentration from zero to 48 pM. The decrease in the absorbance might be due to the formation of insoluble formazan. Although the addition of Triton X-100 improved the solubility of formazan (*12*), precipitates were still observed. The absorbance change observed at 30 min increased from 0.05 to 0.16 with increasing CRP concentration from zero to 48 pM. In addition, the observable absorbance change was considerably smaller than that observed in the EIA system using WST-1 and PMS (Fig. 7), and it was difficult to obtain a calibration curve with the absorbance change at 30 min, because the absorbance was small and not constant. The lowest detection limit of CRP was estimated to be 12 pM (1.2 fmol in 0.1 ml). This indicates that the EIA system using WST-1 and PMS is 40 times more sensitive than the EIA system using INT and diaphorase.

DISCUSSION

Valero *et al.* (*13*) performed kinetic analysis of the enzymatic cycling system in which ADH and diaphorase were used to cycle NAD^+ in the presence of ethanol and INT. They suggest that the cycling system is applicable to EIA to increase the magnitude of the measured response. The EIA system using diaphorase and INT was examined (Fig. 9). However, quantitative results were not obtained because of the formation of insoluble formazan and the instability of diaphorase. Although the addition of Triton X-100 is known to improve the solubility (*12*), the precipitates were still observed. In the present study, the EIA system was improved by replacing INT and diaphorase with WST-1 and PMS, respectively. In the new system, precipitates were not formed. CRP was quantitatively detected with a sensitivity of 50 attomole per well of a micro-titer plate in a 1-h reaction (Figs. 7 and 8). This sensitivity is 24 times higher than that of the system using INT and diaphorase. The sensitivity in a one-enzyme reaction system with ALP using the same combination of anti-CRP antibodies was examined. When PNPP was used as a substrate, the absorbance increase at 405 nm was measured, and the sensitivity was determined to be 50 fmol. With 4-methylumberiferryl phosphate as a substrate, the reaction was followed fluorometrically, and the sensitivity was estimated to be 100 amol. It was suggested that the synchronous EIA using WST-1 and PMS was approximately 1,000 times more sensitive than the conventional EIA with a one-enzyme reaction system with ALP using colorimetric PNPP substrate, and that the sensitivity of the synchronous EIA was similar to that of the conventional EIA using the fluorometric substrate.

In this study, PMS was used instead of diaphorase. The activity of diaphorase varies depending on the lot of the preparation, and the enzyme is fairly unstable. In our experience, its activity decreased to 83% at 5 h and 70% at 8 h after dissolving it in the reaction buffer. Because a long-term reaction would be needed for highly sensitive detection, we tried to use a more stable reagent than diaphorase. PMS, a versatile non-enzymatic electron mediator between NAD(P)H and tetrazolium (*19–21*), retained 93% of its activity at 8 h after dissolving it.

The kinetic theory by Valero *et al.* (*13*) was successfully applied to the (WST-1)-PMS system proposed in this study. The kinetic analysis was useful to understand each reaction in the EIA and to determine the optimal conditions. The formazan concentration during the reaction was given by second-order polynomials of the reaction time (Eq. 15). The rate of formazan formation was determined by k_1 and k (Eq. 22). Although the first-order rate constant k_1 is inherent in ALP (Eq. 18), k is represented by k_2 and k_3, which were expected to increase with increasing ADH and PMS concentrations. The k_1 value was calculated to be 4.37×10^3 min^{-1} in the presence of 50 μM $NADP^+$, and the k_2, k_3, and k values were calculated to be 63.5, 26.3, and 18.6 min^{-1}, respectively, in the presence of 200 μM PMS and 1.6 μM ADH. Under these conditions, CRP was quantitatively detected with a sensitivity of 100 amol per well (0.1 ml) of a micro-titer plate in a 1-h reaction. CRP is one of the most characteristic human acute phase plasma proteins, which is normally a trace constituent (less than 10 nM) but is dramatically increased in the blood within 24 to 48 h in response to inflammatory stimuli (*32, 33*). Thus, the EIA system proposed in this study is sensitive enough for the measurement of CRP in blood, and it is potentially applicable to all kinds of sandwich EIAs for compounds other than CRP.

The background observed in the absence of the analyte was found to diminish the sensitivity of the EIA, and to derive from three major origins. One of them is non-specific binding between the ALP-conjugated antibody and the immobilized mAb. This depends on improper combination between the two antibodies, and it can be eliminated by the selection of more suitable antibodies. We have shown that

the non-specific binding can be much reduced by the use of $F(ab')_2$ fragments in place of the whole antibody molecules, especially when antibodies of the IgM class are used (*4, 5, 34*). The second origin of the background is the contamination of the ADH preparation by ALP. The commercially available ADH preparation contained a small ALP activity, and it was not eliminated completely by HPLC (see below). The third origin is the reduction of PMSox by ADH in the absence of NAD^+. Although it is substantially impossible to eliminate this effect, because both PMS and ADH are essential for the EIA system, its magnitude is negligible in comparison with the background derived from the first and second origins. If these two are removed, the synchronous EIA system proposed in this study (Fig. 1) can be expected to detect fewer than 1,000 molecules of an analyte in a 24-h reaction.

The commercially available preparation of yeast ADH used in this study was homogeneously pure as judged by SDS-PAGE and showed the specific activity of 385–390 U/mg protein. The ADH solution (200 μg/ml), however, exhibited ALP activity equal to 1.75 ng/ml of ALP in the PNPP hydrolysis. The ALP activity contaminating the ADH preparation was regarded as one of the origins of the background formazan formation observed in the absence of the analyte. Therefore, eliminating the ALP activity from the ADH preparation might reduce the background, and this was examined by a combination of hydrophobic interaction HPLC and gel-filtration HPLC on TSKgel Phenyl-5PW and TSKgel $G3000SW_{XL}$ columns, respectively. The purified ADH preparation (200 μg/ml) exhibited ALP activity equal to 1.6–1.7 ng/ml of ALP. This suggests that the ALP contaminating the commercially available ADH preparation was not removed by the HPLC procedures or that the PNPP-hydrolyzing activity was not necessarily due to ALP contaminating the preparation. Therefore, the commercially available ADH preparation as well as the HPLC-purified one was used throughout this study by regarding it as the most suitable ADH preparation with respect to the ALP contamination.

The synchronous EIA system introduced in the present study should be characterized and optimized more precisely for its practical application. Screening and selection of antibodies with higher affinity for the antigen are now continuing. ALP and ADH from other origins are being examined for their applicability to the EIA system. Protein engineering study should also help to improve the functionality of antibodies and enzymes. Data interpretation, assay validation, and quality control (*35*) of the synchronous EIA system and the precise comparison of this system with other EIA systems are under way by collecting a number of assay data.

REFERENCES

1. Tijssen, P. (1985) *Practice and Theory of Enzyme Immunoassays*, pp. 297–504, Elsevier, Amsterdam
2. Diamandis, E.P. and Christopoulos, T.K. (1996) *Immunoassay*, pp. 287–568, Academic Press, San Diego
3. Morimoto, K. and Inouye, K. (1992) Single-step purification of $F(ab')_2$ fragments of mouse monoclonal antibodies (immunoglobulins G1) by hydrophobic interaction high-performance liquid chromatography using TSKgel Phenyl-5PW. *J. Biochem. Biophys. Methods* **24**, 107–117
4. Inouye, K. and Morimoto, K. (1993) Single-step purification of $F(ab')_{2\mu}$ fragments of mouse monoclonal antibodies (immunoglobulins M) by hydrophobic interaction high-performance liquid chromatography using TSKgel Ether-5PW. *J. Biochem. Biophys. Methods* **26**, 27–39
5. Inouye, K. and Morimoto, K. (1994) Preparation of $F(ab')_{2\mu}$ fragments of mouse IgM monoclonal antibodies and their application to the enzyme immunoassay of mouse interleukin-6. *J. Immunol. Methods* **171**, 239–244
6. Inouye, K. and Ohnaka, S. (2001) Pepsin digestion of a mouse monoclonal antibody of IgG1 class formed $F(ab')_2$ fragments in which the light chains as well as the heavy chains were truncated. *J. Biochem. Biophys. Methods* **48**, 23–32
7. Morimoto, K. and Inouye, K. (1997) A sensitive enzyme immunoassay of human thyroid-stimulating hormone (TSH) using bispecific $F(ab')_2$ fragments recognizing polymerized alkaline phosphatase and TSH. *J. Immunol. Methods* **205**, 81–90
8. Inouye, K. (1997) Bispecific-Ab-based immunoassay of thyroid-stimulating hormone. *Cancer Immunol. Immunother.* **45**, 159–161
9. Morimoto, K. and Inouye, K. (1999) Method for the preparation of bispecific $F(ab')_{2\mu}$ dfragments from mouse monoclonal antibodies of the immunoglobulin M class and characterization of the fragments. *J. Immunol.Methods* **224**, 43–50
10. Stanley, C.J., Johannsson, A., and Self, C.H. (1985) Enzyme amplification can enhance both the speed and the sensitivity of immunoassays. *J. Immunol. Methods* **83**, 89–95
11. Self, C.H. (1985) Enzyme amplification-A general method applied to provide an immunoassisted assay for placental alkaline phosphatase. *J. Immunol. Methods* **76**, 389–393
12. Johannsson, A., Ellis, D.H., Bates, D.L., Plumb, A.M., and Stanley, C.J. (1986) Enzyme amplification for immunoassays. Detection limit of one hundredth of an attomole. *J. Immunol. Methods* **87**, 7–11
13. Valero, E., Varón, R., and García-Carmona, F. (1985) Kinetic study of an enzymic cycling system coupled to an enzymic step. Determination of alkaline phosphatase activity. *Biochem. J.* **309**, 181–185
14. Brooks, J.L., Mirhabibollahi, B., and Kroll, R.G. (1990) Sensitive enzyme-amplified electrical immunoassay for protein A-bearing *Staphylococcus aureus* in foods. *Appl. Environ. Microbiol.* **56**, 3278–3284
15. Vera-Cabrera, L., Handzel, V., and Laszlo, A. (1994) Development of an enzyme-linked immunosorbent assay (ELISA) combined with a streptavidin-biotin and enzyme amplification method to detect anti-2,3-di-*o*-acyltrehalose (DAT) antibodies in patients with tuberculosis. *J. Immunol. Methods* **177**, 69–77
16. Wicks, B., Cook, D.B., Barer, M.R., O'Donnell, A.G., and Self, C.H. (1998) A sandwich hybridization assay employing enzyme amplification for determination of specific ribosomal RNA from unpurified cell lysates. *Anal. Biochem.* **259**, 258–264
17. Ishiyama. M., Shiga, M., Sasamoto, K., Mizoguchi, M., and He, P. (1993) A. new sulfonated tetrazolium salt that produces a highly water-soluble formazan dye. *Chem. Pharm. Bull.* **41**, 1118–1122
18. Ukeda, H., Kawana, D., Maeda, S., and Sawamura, M. (1999) Spectrophotometric assay for superoxide dismutase based on the redution of highly water-soluble tetrazolium salts by xanthine-xanthine oxidase. *Biosci. Biotechnol. Biochem.* **63**, 485–488
19. Nakamura, S., Arimura, K., Ogawa, K., and Yagi, T. (1980) Use of 1-methoxy-5-methylphenazinium methyl sulfate (1-methoxy PMS) in the assay of some enzymes of diagnostic importance. *Clin. Chim. Acta* **101**, 321–326
20. Hisada, R. and Yagi, T. (1977) 1-Methoxy-5-methylphenazinium methyl sulfate. *J. Biochem.* **82**, 1469–1473
21. Obón, J.M., Buendía, B., Cánovas, M., and Iborra, J.L. (1999) Enzymatic cycling assay for D-carnitine determination. *Anal. Biochem.* **274**, 34–39
22. Abe, N. and Inouye, K. (1993) Purification of monoclonal antibodies with light-chain heterogeneity produced by mouse hybridomas raised with NS-1 myelomas: Application of hydrophobic

interaction high-performance liquid chromatography. *J. Biochem. Biophys. Methods* **27**, 215–217
23. Inouye, K. and Gohzu, S. (1991) Separation of mouse immunoglobulin G subclasses by high-performance liquid chromatography. *Agric. Biol. Chem.* **55**, 2161–2162
24. Lowry, O.H., Rosebrough, N.J., Farr, A.L., and Randall, R.J. (1951) Protein measurement with the Folin phenol reagent. *J. Biol. Chem.* **193**, 265–275
25. Henthorn, P.S., Raducha, M., Edwards, Y.H., Weiss, M.J., Slaughter C., Lafferty, M.A., and Harris, H. (1987) Nucleotide and amino acid sequences of human intestinal alkaline phosphatase. Close homology to placental alkaline phosphatase. *Proc. Natl. Acad. Sci. USA* **84**, 1234–1238
26. Worthington, C.C. (1988) *The Worthington Manual*, pp. 16–24, Worthington Biochemical Co., Freehold, N.J.
27. Bennetzen, J.L. and Hall, B.D. (1982) The primary structure of the Sacchaaromyces cerevisiae gene for alcohol dehydrogenase I. *J. Biol. Chem.* **257**, 3018–3025
28. Worthington, C.C. (1988) *The Worthington Manual*, pp. 137–139, Worthington Biochemical Co., Freehold, N.J.
29. Oneda, H. and Inouye, K. (2001) Interaction of human matrix metalloproteinase 7 (matrilysin) with the inhibitors thiorphan and R-94138. *J. Biochem.* **129**, 429–435
30. Parkes, C. and Abeles, R.H. (1984) Studies on the mechanism of action of methoxatin-requiring methanol dehydrogenase. Reaction of enzyme with electron-acceptor dye. *Biochemistry* **23**, 6355–6363
31. Fox, M.G.A., Dickinson, M., and Ratledge, C. (1992) Long-chain alcohol and aldehyde dehydrogenase activities in *Acinetobacter calcoaceticus* strain HO1-N. *J. Gen. Microbiol.* **138**, 1963–1972
32. Miyazawa, K. and Inoue, K. (1990) Complement activation induced by human C-reactive protein mildly acidic conditions. *J. Immunol.* **145**, 650–654
33. Pepys, M.B. and Baltz, M.L. (1983) Acute phase proteins with special reference to C-reactive protein and related proteins (pentaxins) and serum amyroid A protein. *Adv. Immunol.* **34**, 141–212
34. Morimoto, K. and Inouye, K. (1997) Flow cytometric analysis of sialysl Lewis A antigen on human cancer cells by using $F(ab')_{2\mu}$ fragmentsa prepared from a mouse IgM monoclonal antibody. *Cytotechnology* **24**, 219–226
35. Grotjan, H.E. and Keel, B.A. (1996) Data Interpretation and Quality Control in *Immunoassay* (Diamandis, E.P. and Christopoulos, T.K., eds.) pp. 51–93, Academic Press, New York